Biomaterials 67 (2015) 11–19

Contents lists available at ScienceDirect

Biomaterials

journal homepage: www.elsevier.com/locate/biomaterials

Rapidly light-activated surgical protein glue inspired by mussel adhesion and insect structural crosslinking

Eun Young Jeon [a, 1], Byeong Hee Hwang [a, b, 1], Yun Jung Yang [a], Bum Jin Kim [a], Bong-Hyuk Choi [a], Gyu Yong Jung [c], Hyung Joon Cha [a, *]

[a] Department of Chemical Engineering, Pohang University of Science and Technology, Pohang 790-784, South Korea
[b] Division of Bioengineering, Incheon National University, Incheon 406-772, South Korea
[c] Department of Plastic Surgery, College of Medicine, Dongguk University, Gyeongju 780-714, South Korea

ARTICLE INFO

Article history:
Received 1 April 2015
Received in revised form
4 July 2015
Accepted 10 July 2015
Available online 14 July 2015

Keywords:
Mussel adhesive protein
Protein adhesive
Tissue adhesive
Light-activated hydrogel
Dityrosine crosslinks

ABSTRACT

Currently approved surgical tissue glues do not satisfy the requirements for ideal bioadhesives due to limited adhesion in wet conditions and severe cytotoxicity. Herein, we report a new light-activated, mussel protein-based bioadhesive (LAMBA) inspired by mussel adhesion and insect dityrosine crosslinking chemistry. LAMBA exhibited substantially stronger bulk wet tissue adhesion than commercially available fibrin glue and good biocompatibility in both *in vitro* and *in vivo* studies. Besides, the easily tunable, light-activated crosslinking enabled an effective on-demand wound closure and facilitated wound healing. Based on these outstanding properties, LAMBA holds great potential as an ideal surgical tissue glue for diverse medical applications, including sutureless wound closures of skin and internal organs.

1. Introduction

A sutureless wound closure is essential to simplify surgical procedures and improve patient care quality. Traditionally, mechanical fasteners like sutures and staples have been used in 60% of rejoining tissues [1]. However, they are not always suitable, especially for preventing the leakage of air or bodily fluids and for suturing friable tissues and non-accessible organs. They can also cause severe tissue damage due to localized stress and need suture removal. Therefore, tissue adhesives are being pursued to overcome the obstacles and promote wound healing without penetration [2]. Despite intensive studies, a perfect bonding material has not yet been developed, and current available options have significant limitations. For example, cyanoacrylates, a chemically derived representative, have toxicity [3]. Biologically derived fibrin glue has limited tissue adhesion [4]. Moreover, most developed glues are easily washed out in a wet environment due to poor mechanical properties or long curing times [5].

Fortunately, nature has provided a captivating source for ideal tissue glue, namely mussel adhesive proteins (MAPs) [6]. Mussels can stably fix their body to wet surfaces with byssal threads. To understand mussel adhesion mechanisms, six distinct MAPs, i.e., foot protein type 1 (fp-1) to foot protein type 6 (fp-6), have been identified from byssal plaques, and 3,4-dihydroxy-phenylalanine (DOPA) residues in natural MAPs have been considered as a key factor for strong underwater adhesion [7,8,10]. Previously, to overcome limited applications due to the extreme difficulty in preparing natural MAPs, hybrid-type recombinant MAP was newly designed and successfully mass-produced in bacterial system [8,9]. This recombinant MAP has proven to be flexible, biodegradable, biocompatible, and strongly adhesive on various surfaces [9,11]. However, due to the intrinsic inabilities of a bacterial system such as lack of post-translational modifications, enzyme-mediated DOPA modification step is required to prepare DOPA-containing recombinant MAP. It is essential to address current challenges of low modification yield and DOPA-containing MAP instability [12,13]. Therefore, a direct use of recombinant MAP without modification would be a facile and economical alternative for MAP-based medical applications such as surgical wound closure.

Herein, to develop a rapidly acting surgical protein glue creating stable adhesive and cohesive bonds without DOPA modification, we utilized a dityrosine photo-crosslinking strategy in recombinant

* Corresponding author.
E-mail address: hjcha@postech.ac.kr (H.J. Cha).
[1] These two authors contributed equally to this work.

http://dx.doi.org/10.1016/j.biomaterials.2015.07.014
0142-9612/

MAP. In insect structural proteins including resilins of dragonfly wings [14], fibroins of silk worms [15], and locust cuticles [16], dityrosine crosslinks are expected to occur spontaneously between tyrosine residues via photo-oxidation reaction. Because dityrosine crosslinks are known to confer mechanical and conformational stability and elasticity to protein chains [17], their introduction into tyrosine-rich (approximately 20 mol%) MAP may significantly increase structural support and adhesive properties as a very stable bridge. Additionally, the use of a visible light is anticipated for controllable, safe, and rapid wound closures. Therefore, we evaluated the novel concept (Fig. 1) of a light-activated mussel protein-based bioadhesive (LAMBA) as an ideal tissue glue via *in vitro* and *in vivo* studies.

2. Materials and methods

2.1. Preparation of recombinant hybrid MAP

Recombinant hybrid MAP fp-151, which is comprised of six fp-1 decapeptide repeats at both the N- and C-termini of fp-5, was produced in an *Escherichia coli* system as previously reported [9]. In brief, transformed *E. coli* BL21 (DE3) cells were cultured in 5 L Luria–Bertani (LB) medium containing 50 μg/mL ampicillin (Sigma) at 37 °C and 300 rpm. At an optical density of 0.4–0.6 at 600 nm, 1 mM isopropyl-β-D-thiogalactopyranoside (IPTG; Sigma) was added to the medium to induce the expression of recombinant MAP. The cells were subsequently incubated for another 8 h at 37 °C and 300 rpm. After centrifugation of the broth at 9000 × g for 10 min at 4 °C, the cell pellets were suspended in 15 mL lysis buffer (10 mM Tris–HCl and 100 mM sodium phosphate; pH 8.0) per gram wet weight. The cells were lysed with constant cell disruption systems (Constant Systems) at 20 kpsi. The lysates were centrifuged at 9000 × g for 20 min at 4 °C, and isolated inclusion bodies were treated with Triton X-100 washing buffer (1% (v/v) Triton X-100 (Sigma), 1 mM EDTA, and 50 mM Tris–HCl; pH 8.0) with 10 mM phenylmethanesulfonyl fluoride (PMSF; Sigma) and 1 mg/mL lysozyme (Bio Basic) and agitated overnight. After centrifugation, the inclusion bodies were resuspended in Triton X-100 washing buffer and then resuspended in 40 mL of 25% (v/v) acetic acid per gram wet weight to extract recombinant MAP with relatively high purity (~97%) [9]. The extracted solution was centrifuged at 9000 × g for 20 min at 4 °C, and the supernatant was collected, dialyzed in deionized water (DW), and then lyophilized.

2.2. Photochemical crosslinking for fabrication of LAMBA hydrogels

To couple two adjacent tyrosine residues into a dityrosine adduct, we employed a well-established photo-oxidative reaction involving the activation of a ruthenium complex, Ru(II)bpy$_3^{2+}$, with an electron acceptor (e.g., sodium persulfate; SPS) in the presence of blue light [18]. Briefly, fresh stock solutions of 50 mM Ru(II)bpy$_3^{2+}$ (Sigma) and 500 mM SPS (Sigma) were prepared via dissolution in DW, respectively. Mixtures of recombinant MAP, 2 mM Ru(II)bpy$_3^{2+}$, and 10–30 mM SPS in 200 mM sodium acetate buffer (pH 5.5) were dispensed into Teflon molds or tip-removed 1 mL syringes and irradiated for 60 s at room temperature with an LED dental curing lamp (460 nm, 1200 mW/cm^2; FORZA4) from a distance of 20 mm.

2.3. Detection of dityrosine links in LAMBA hydrogels

The presence of dityrosine and dityrosine-like compounds in fabricated LAMBA hydrogel after the photochemical crosslinking reaction was evaluated via the fluorescence detection of acid hydrolysates [19]. These compounds have particular emissions at 410 nm when excited at 315 nm. To induce the full hydrolysis of amide bonds, 10 μL hydrogel sample with 2 mg MAP was reacted with 1 mL of 6 N HCl in a sealed 1.5 mL centrifuge tube in a heat block at 105 °C for 2 h. Then, 100 μL of acid hydrolysis product was transferred to a new 1.5 mL centrifuge tube and neutralized with 5 M NaOH. Then, 100 mM Na_2CO_3–$NaHCO_3$ buffer (pH 9.9) was added to the tube to a 1 mL final volume. To confirm the crosslinking density of the hydrogels made with different SPS concentrations, the fluorescence spectra of the samples were measured. The yields of the dityrosine and dityrosine-like products in the hydrogels were quantified according to the fluorescence concentration standard curve of purified dityrosine.

2.4. Surface morphology analysis of LAMBA hydrogel

The photochemically crosslinked hydrogels were equilibrated in DW for 24 h and then lyophilized for 2 days. The swollen, freeze-dried samples were cross-sectioned, mounted on an aluminum substrate, and sputter-coated with gold for 40 s. The internal structures of the gel specimens were investigated via scanning electron microscopy (SEM; JEOL) at 5.0 kV.

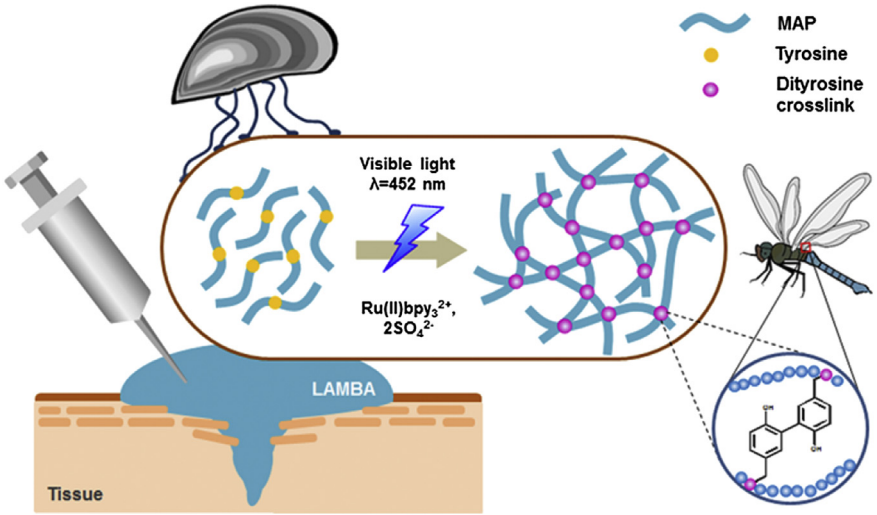

Fig. 1. Schematic representation of recombinant MAP-based bioadhesive formation via dityrosine bonds using visible light.

2.5. Measurement of dynamic swelling kinetics

Cast discs (5 mm diameter × 3.5 mm height) of the hydrogels were weighed after drying for 24 h (Wi) and then immersed in phosphate-buffered saline (PBS) at 37 °C. At predetermined intervals ranging from 0.5 to 60 h, the swollen samples were blotted on paper towels to remove the buffer from the surface and then weighed again (Ws). The swelling ratio was calculated using the following equation: swelling ratio (%) = [(Ws-Wi)/Wi] × 100, where Ws is the weight of the swollen sample and Wi is the weight of the dried sample.

2.6. Measurement of elastic modulus

The elastic moduli of the photo-crosslinked LAMBA hydrogels were obtained via unconfined, uniaxial compression tests using a universal testing machine (Instron) equipped with a 10 kN load cell. Cylindrical-shaped samples were prepared as described above and immersed in DW for 24 h to reach equilibrium swelling states. Their diameters and thicknesses were measured using calipers, and they were compressed at a rate of 0.01 mm/s until the strain reached 35%. The compressive elastic modulus was determined from the slope of the linear region in the 0–15% strain range of the stress–strain curve. For each measurement, six samples were averaged to obtain the modulus.

2.7. Measurement of tissue adhesive strength in a wet environment

To assess the wet tissue adhesive strength, we performed lab shear tests using the universal testing machine. Porcine skins (Stellen Medical), used as tissue substrates, were cut and bonded onto transparent acrylic fixtures using cyanoacrylate glue (3M). Pre-hydrogel solution was spread on one surface of the porcine skin, and the specimen was covered with the other tissue specimen to form a bonding area of 10 × 10 mm^2. Then, the adhered substrates were immediately irradiated using a dental curing lamp for 60 s to crosslink the solution to form a hydrogel between two tissue specimens. After curing, the sample was immersed in PBS at room temperature for 2 h prior to measurement. The bonded samples were loaded until complete separation at a crosshead speed of 5 mm/min with a 10 kN load cell. The results from six samples were averaged to obtain each measurement. The wet tissue adhesive strengths of 30% (w/v) original MAP solution and fibrin glue (Tisseel®; Baxter) were also measured as comparative controls.

2.8. Cytocompatibility assay of LAMBA hydrogels

The *in vitro* cytotoxicity of pre-hydrogel solution was quantitatively determined using a Cell Counting Kit-8 assay (CCK-8; Dojindo). LAMBA pre-hydrogel solutions in Dulbecco's modified Eagle's medium (DMEM; Hyclone) containing 10% (v/v) fetal bovine serum (FBS; Hyclone) and 1% (v/v) streptomycin (Hyclone) were prepared at three different concentrations: 10, 1, and 0.1 mg/mL. Then, HaCaT keratinocyte cells in DMEM at a concentration of 4 × 10^3 cells per well were added into each well of a 96-well cell culture plate and incubated for 24 h at 37 °C and 5% CO_2. Then, the media was replaced with the prepared media and the different pre-hydrogel solutions. These were cultured for another 48 h. Cell viability was evaluated via CCK-8 assay, and the results were normalized to that of cells grown in blank medium as a negative control. The cytocompatibility of crosslinked LAMBA was also evaluated using gel extracts obtained from the hydrogel using DMEM at an extraction ratio of 15 mg/mL for 24 h at 37 °C [20]. HaCaT cells were seeded at 4 × 10^3 cells per well and cultured for 24 h. After incubation, the supenatant of each well was replaced with the gel extracts, which were then incubated for another 24 and 48 h at 37 °C and 5% CO_2. The CCK-8 assay was performed to assess cell viability, and the blank medium and 10% dimethyl sulfoxide (DMSO) were compared as negative and positive controls, respectively.

2.9. In vivo wet wound closure using a rat skin incision wound model

All animal studies were carried out in accordance with guidelines by national regulations and the approval of the local Institutional Animal Care and Use Committee (2013-01-0027). To assess the *in vivo* wet wound closure and biocompatibility of LAMBA, normal Sprague Dawley (SD) rats were anesthetized. After shaving, deep, 2-cm-long incisions were made on the skin of the back. With the exception of the untreated control group, each wound was treated via suture, fibrin glue (Tisseel®), cyanoacrylate (Dermabond®; Ethicon) or LAMBA hydrogel using 30% (w/v) MAP and 30 mM SPS. The closured skins were harvested on day 0, 7, and 14 of the experimental period after CO_2 euthanization. The collected skin (3 × 3 cm) was utilized for both mechanical strength measurements and histological analysis. To measure the wound breaking strength of the rejoined tissue, a 1 × 3-cm section of the skin was loaded on the universal testing machine with a 10 kN load cell and a crosshead speed of 5 mm/min. For histological analysis via hematoxylin and eosin (H&E) staining, the remaining skin section was fixed in 10% buffered formalin (Sigma). To confirm collagen synthesis, Masson's trichrome (MT) staining was performed. All imaging analyses were performed on a Leica microscope (Leica; Wetzlar).

2.10. Statistical analysis

All data are presented as the means ± standard deviations. The significance of differences between results was assessed via one-way ANOVA.

3. Results and discussions

3.1. Light-activated formation of adhesive hydrogel using recombinant MAP

To confer mechanical stability to unmodified tyrosine-rich MAP, ruthenium-based photochemistry was employed by coupling two nearby tyrosine residues [18]. The proposed mechanism suggests photolyzed ruthenium-mediated formation of a tyrosyl radical, coupling with nearby tyrosine residue, and subsequent removal of a hydrogen atom by a sulfate radical. A light-responsive crosslinking is of particular interest due to easy accessibility, homogeneous crosslinking, and mild conditions (e.g., physiological temperatures). In contrast, most chemical crosslinking can induce a large-scale modification of proteins, resulting in structural destabilization and inflammation by exposure to toxic organic solvents and crosslinking reagents like glutaraldehyde and carbodiimide [21].

For optimal gelation, 10–30% (w/v) MAP was used because less than 5% (w/v) solution could not be solidified. Ru(II)bpy_3^{2+} was set at a low concentration of 2 mM because this catalyst is recycled during photochemical reaction. The amount of SPS was maintained below 40 mM to avoid self-aggregation of protein. Through optimization, MAP solution was rapidly crosslinked into a gel with desired shape within 60 s via irradiation (Fig. 2a, left upper image).

The presence of dityrosine in LAMBA after photo-crosslinking was confirmed by their characteristic blue fluorescence under UV illumination. LAMBA containing dityrosine showed a distinct blue

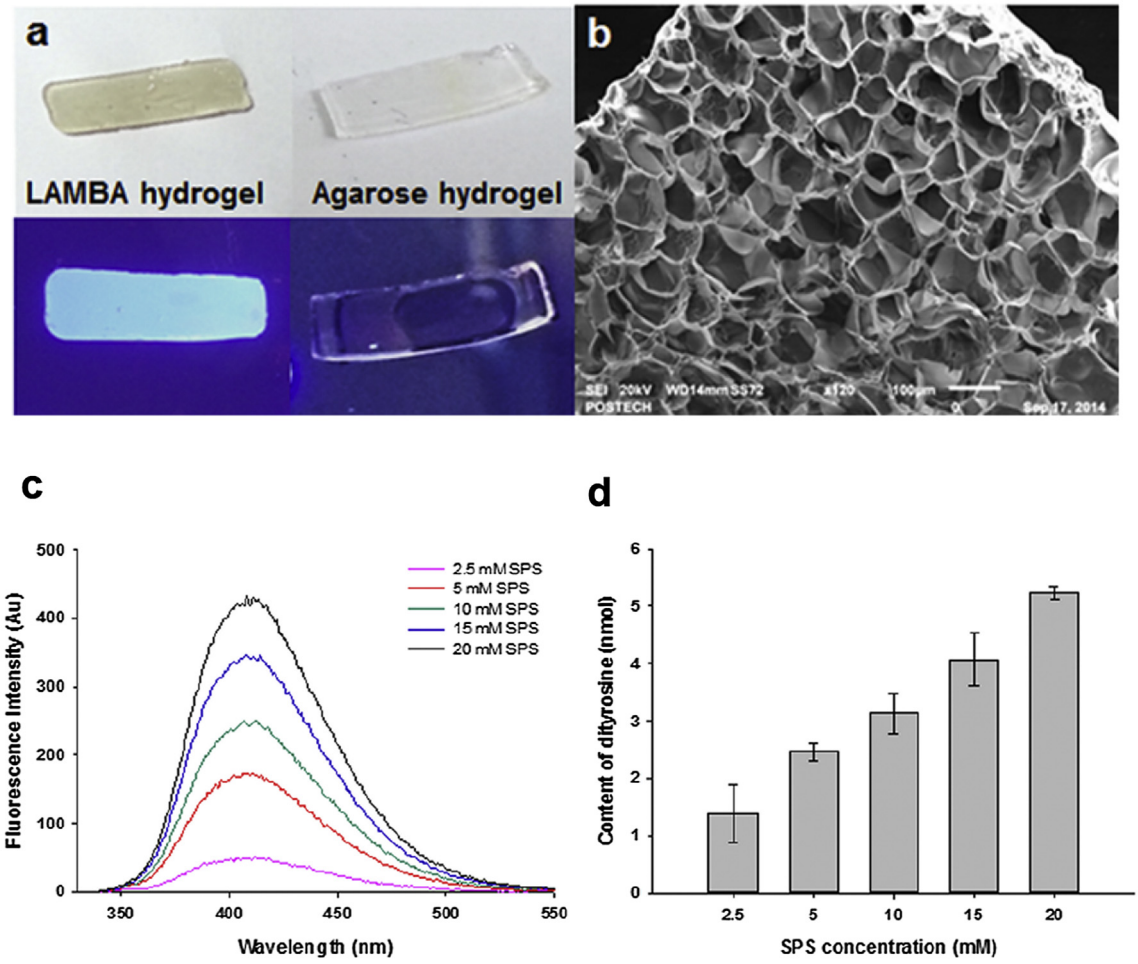

Fig. 2. a) Photographs of LAMBA (left) containing dityrosine adducts and agarose gel (right) as a comparative control under room light (top) and UV illumination (bottom). b) SEM analysis of microporous structure of LAMBA hydrogel with 30% (w/v) MAP and 20 mM SPS. c) Fluorescence spectra of the acid hydrolysis products of LAMBA hydrogels with different SPS concentrations. d) Yield of dityrosine products in 10 μL LAMBA hydrogels with 2 mg MAP. Triplicate samples were averaged to obtain the results for each measurement.

fluorescence (Fig. 2a, left lower image), whereas the control gel did not (Fig. 2a, right lower image). In the fluorescence spectra of the acid hydrolysis products of LAMBA, a particular emission peak at 410 nm was observed, which is a value attributed to purified dityrosine (Fig. 2c). Moreover, based on the fluorescence standard curve of purified dityrosine, the amount of formed dityrosine in 10 μL hydrogel was quantified (Fig. 2d). More tyrosine residues were likely converted to dityrosine crosslinks by increasing SPS content. This is because persulfate radicals produced during photolysis of $Ru(II)bpy_3^{2+}$ play a key role in removing hydrogen atoms to produce highly stable dityrosine crosslinks [18].

3.2. Physical properties of LAMBA hydrogels

Images of SEM revealed the internal structure of LAMBA. LAMBA showed a highly porous 3D scaffold that was interconnected via intra- and inter-molecular crosslinking (Fig. 2b), which can provide favorable environments for natural cell behavior. The pore size was tunable from 42.1 ± 5.4 μm to 301.7 ± 37.5 μm by adjusting SPS content (data not shown). This meets the range for the regeneration of adult mammalian skin (i.e., 20–125 μm) [22].

To evaluate swelling kinetics of LAMBA in physiological condition, LAMBA hydrogels with different SPS and MAP contents were incubated in PBS for 60 h. In all hydrogels tested, they rapidly swelled and reached equilibrium states within 5 h (data not shown). The equilibrium swelling ratio decreased from 314 ± 12% to 210 ± 13% as SPS content increased (Fig. 3a). The higher SPS content led to more arene couplings and denser crosslinked network, which resulted in the lower swelling ratio. By increasing MAP content, the effect of tyrosine levels on ultimate swelling ratio was also investigated (Fig. 3b). The value was reduced from 263 ± 15% to 202 ± 11% due to an increase of crosslinkable phenolic moieties and decreased molecular chain flexibility. In sutureless wound closures, such controllable swelling can be a great asset, especially in wound healing by providing a highly permeable flexible seal for removal of exudates and a facilitated mass transfer for cellular functions [23].

Next, LAMBA were subjected to uniaxial, unconfined compression tests to determine mechanical properties. LAMBA constructed from 20% (w/v) MAP showed a gradual increase in compressive elastic modulus from 37.1 ± 1.8 kPa to 99.5 ± 14.9 kPa as SPS content increased (Fig. 3c). Similarly, for LAMBA formulated with 30 mM SPS, elevating MAP content resulted in an improved modulus from 33.0 ± 5.6 kPa to 144.7 ± 18.0 kPa (Fig. 3d). Thus, by controlling crosslinking degree (i.e., altering SPS and/or MAP content), the mechanical properties of LAMBA can be easily modulated. A broad mechanical moduli range of LAMBA can be advantageous when applied to tissues with varying elastic moduli, including 260–490 Pa for brain [24], ~640 Pa for liver [25], and ~66 kPa for breast [26].

To investigate the bulk tissue adhesive strength of LAMBA in wet

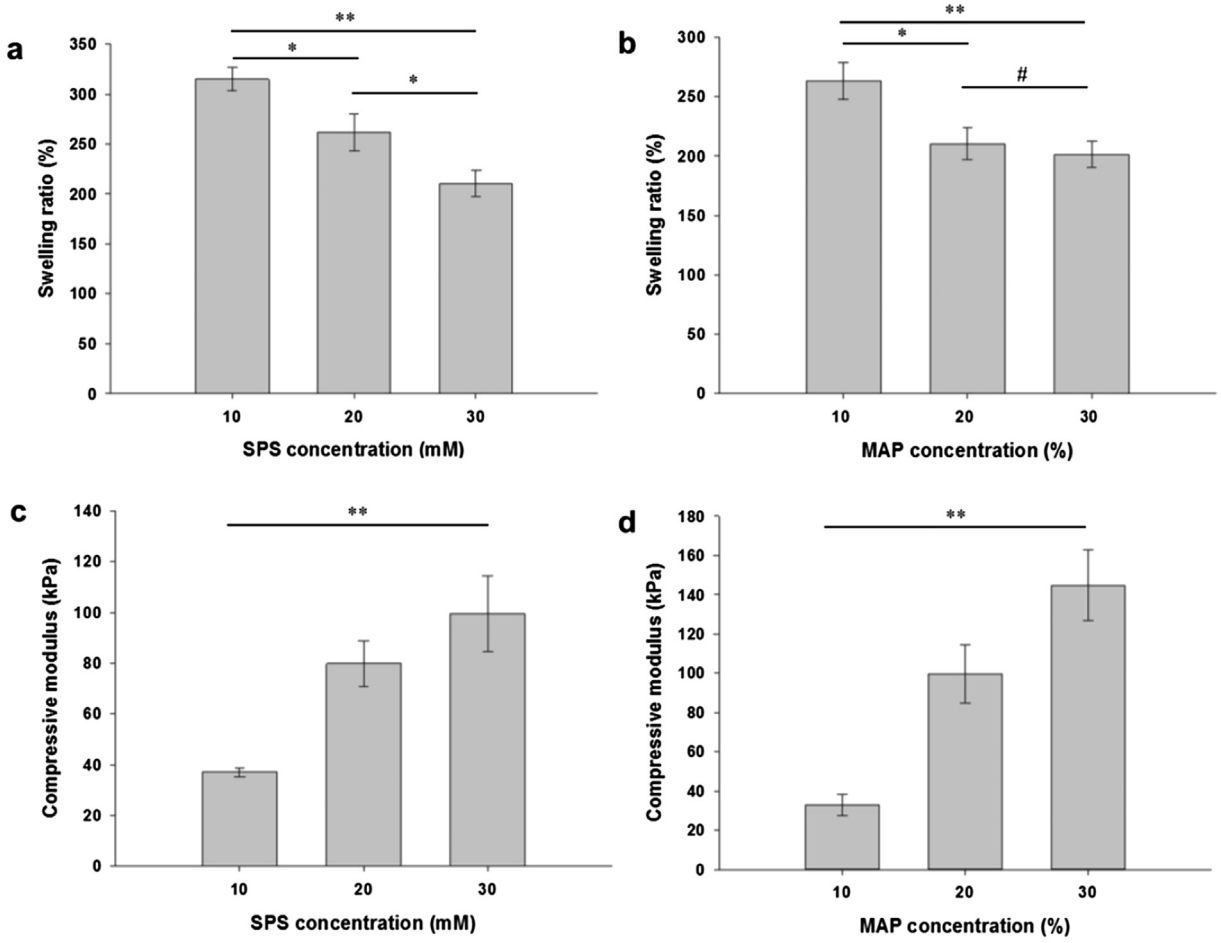

Fig. 3. Swelling ratio of various hydrogels with different a) SPS and b) MAP concentrations was obtained at equilibrium. Three independent samples were averaged to obtain each measurement. Compressive moduli of LAMBA hydrogels were determined by changing the c) SPS and d) MAP concentrations. Six independent samples were averaged to obtain each measurement. Statistical significance is designated (**$p < 0.01$, *$p < 0.05$, and #$p > 0.05$.).

condition, *in vitro* lap shearing test was performed using porcine tissue as a substrate. For measurement, the attached porcine skins by photo-crosslinked LAMBA were promptly immersed in PBS for 2 h (Fig. 4a). As expected, LAMBA made with 30% (w/v) MAP showed superior tissue adhesive strength to that of 30% (w/v) original MAP solution by a factor of 2.2-fold. In an aqueous condition, the crosslinked LAMBA retained a solidified, rigid form, whereas the non-crosslinked MAP was easily lost during immersion. There were no significant differences between wet tissue adhesive strengths of 30% (w/v) original MAP (22.3 ± 5.5 kPa) and fibrin glue (20.2 ± 3.4 kPa). However, LAMBA provided excellent adhesiveness: 33.5 ± 8.8 kPa for 20% (w/v) MAP and 48.2 ± 10.1 kPa for 30% (w/v) MAP. Furthermore, the maximum strength of LAMBA (72.2 ± 3.7 kPa) was determined when using 50% (w/v) MAP (data not shown). Great tissue adhesion of LAMBA is likely correlated with tyrosine content in MAP; tyrosine residues are involved in 1) cohesive integrity via intermolecular dityrosine crosslinks and 2) additional surface adhesiveness with nearby tyrosine residues of the extracellular matrix (ECM) proteins in treated tissues during photo-crosslinking [18]. Besides, cation-π interaction and π-π stacking can account for important parts of the adhesion, which was reported the main interaction for underwater adhesion of green mussels [27–29]. Because MAP was characterized to be cationic polyelectrolyte containing almost equal amounts of both aromatic residues (e.g., tyrosine ~22 mol%) and cationic residues (e.g., lysine ~20 mol%) [9], such cation-π interaction and/or π-π stacking can occur both inside LAMBA and at the LAMBA-tissue interface under physiological condition.

3.3. Cytocompatibility of LAMBA hydrogels

Ideal biomaterials should not cause cytotoxicity. The cytotoxicities of the pre-hydrogel solution and the leachable content of LAMBA were evaluated using keratinocyte HaCaT cells. After 48 h culture with 10 mg/mL pre-hydrogel solution, the cell viability was between 70.6 ± 3.6% and 86.0 ± 1.4% relative to that in a blank medium (Fig. 5a). In diluted pre-hydrogel solutions, the viabilities were comparable with that of the negative control. Furthermore, the cytotoxicity of hydrogels was assessed by contacting the gel extracts directly with cells. The cell viabilities in the gel extracted medium after 24 and 28 h culture were normalized to that of the negative control at 24 h (Fig. 5b). More than 90% of cells were viable after 24 h, and a value higher than the negative control viability was shown after 48 h incubation. This indicated a negligible potential cytotoxicity of the gel extracts. Previously, $Ru(II)bpy_3^{2+}$ showed no cytotoxicity on fibroblast at routinely used concentrations [30]. Although SPS was relatively cytotoxic, more than 99% of SPS content was rapidly consumed during the reaction, and the remains did not cause cytotoxicity [30]. As a light source, visible light is more cytocompatible for *in situ* biomaterials compared with UV light because cells contain many molecules absorbing UV light and few visible chromophores [31].

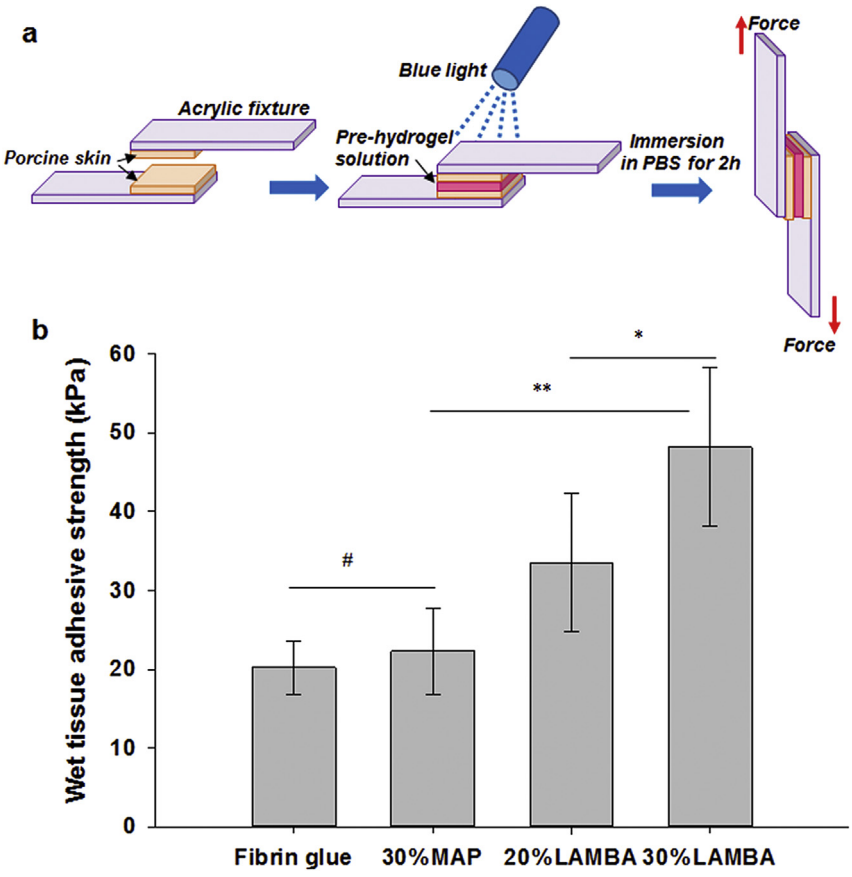

Fig. 4. a) Schematic of lab shearing test setup to measure tissue adhesive strength using porcine skins. b) Wet tissue adhesive strengths of fibrin glue, non-crosslinked MAP, and LAMBA. Six independent samples were averaged to obtain each measurement (**p < 0.01, *p < 0.05, #p > 0.05).

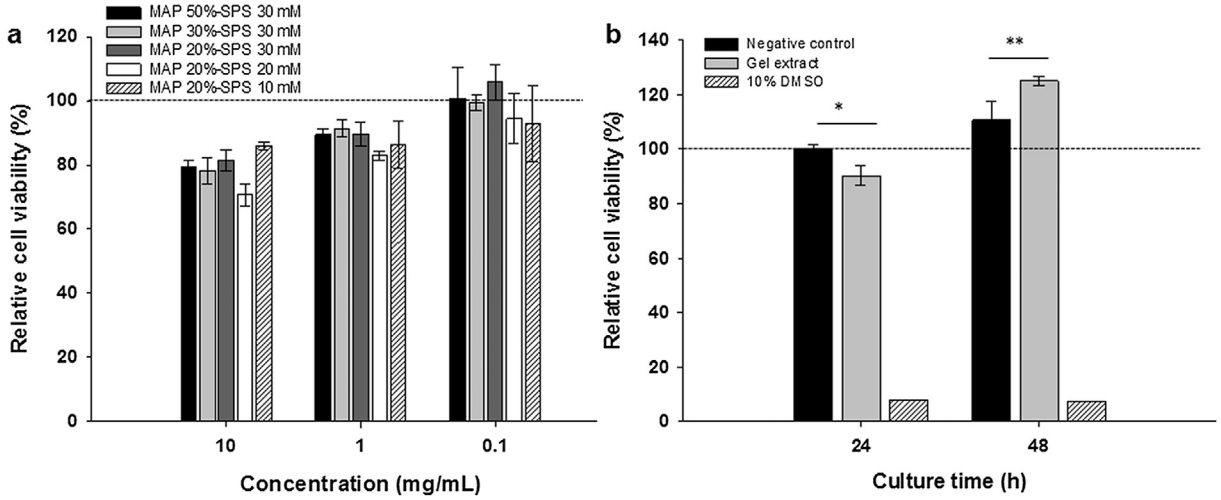

Fig. 5. *In vitro* cytotoxicity of LAMBA hydrogels was evaluated using HaCaT keratinocyte cells. a) After incubation in the medium including pre-hydrogel solution for 48 h, relative cell viabilities were determined by normalizing the values (100%) to cell viability in blank medium at 48 h. Seven independent samples were averaged to obtain each measurement. b) Cell viabilities in the gel extracts were normalized to the cell viability (100%) of a negative control at 24 h. Six samples were averaged to obtain each measurement. Statistical significance is designated (**p < 0.01, *p < 0.05, and #p > 0.05).

3.4. *In vivo* rat skin incision wound closure using LAMBA

To explore the effectiveness and convenience of LAMBA as a rapid surgical glue, incisions on the back of a rat were untreated and treated with suture, fibrin glue, cyanoacrylate, and LAMBA. All animal studies were performed by the approval of the local Institutional Animal Care and Use Committee. Immediately after the treatments, complete wound closures were observed for all groups except for the untreated case (Fig. 6a). During the treatments, cyanoacrylate did not adhere to the incision site and was free-

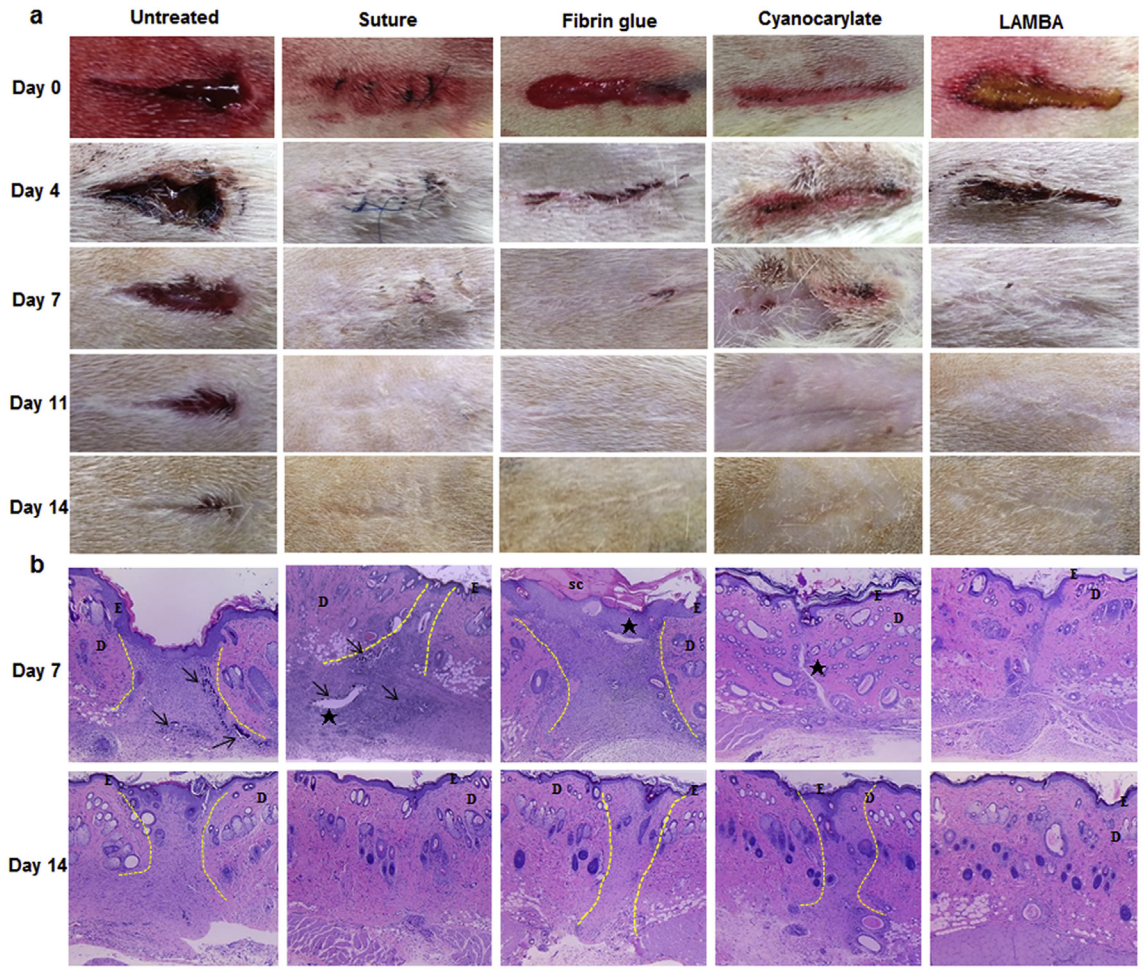

Fig. 6. a) Images of rat incisions untreated or treated with suture, fibrin glue, cyanoacrylate, and LAMBA. b) Images of wounded tissues stained with H&E staining. Epidermis (E), dermis (D), scab (sc), tissue defect (★), fibrosis (black arrow), and wound site (yellow dashed-line) are indicated. (For interpretation of the references to colour in this figure legend, the reader is referred to the web version of this article.)

flowing until curing. Fibrin glue on the bleeding site was easily washed out due to relatively slow gelation. However, upon light irradiation, LAMBA solution was rapidly cured and closed the wound within 60 s with easy handling. Afterward, no blood leakage was observed unlike suture-treated incisions. At day 7, LAMBA appeared to be fully degraded via proteolysis, and hair regrew across the incision with minimal scarring. In contrast, solid impermeable covers remained on cyanoacrylate-treated wound, which caused a hairless wound site and a clear rejoining mark after detachment of the hard glue surface. Untreated tissue clearly showed a subsequent gap between the anchoring edges.

Histological analyses using H&E staining showed that the LAMBA-treated tissue had effective reepithelialization, significant reductions in the wound area, and only minor inflammation compared with the other groups at day 7 (Fig. 6b). The untreated tissue displayed signs of fibrosis and inflammation without newly remodeled dermis. The fibrin glue-treated wound also showed an incomplete dermis recovery and presented with scab. Although the suture and cyanoacrylate treatments showed better wound closure and reepithelialization than fibrin glue, tissue defects in the dermis were observed. At day 14, prolonged and intense inflammations were evident in the untreated and cyanoacrylate-covered incisions, which can delay a phenotypic transition to a reparative state, leading to impaired healing and ECM collapse [32,33]. The fibrin glue-treated skin still showed a loose tissue arrangement due to deficient wound healing. Importantly, the LAMBA-treated wound displayed restored skin morphology without visible fibrosis and inflammation at the wound site, which indicates that LAMBA treatment promoted the transition from inflammatory phase to proliferative phase of healing. The mild and minimal inflammation for effective healing is likely attributed to the previously reported biocompatible nature of MAP including efficient adhesion for various cell types [9].

To assess the deposition of newly produced collagen at the incision site, the healed tissues were analyzed with MT staining, which dyes collagen blue (Fig. 7a). In wound healing, collagen fiber plays a dominant role in restoring structure and function [32,33]. At day 7, poor tissue reconstruction was observed in the untreated and fibrin glue-treated skins. Collagen density in the suture-treated incision was less than that in the LAMBA-treated case. At day 14, a more organized tissue structure was observed in the LAMBA-treated wound. Compared to rigid and dry surfaces of other adhesives such as scab of fibrin glue and cover of cyanoacrylate, LAMBA could keep the wound site moist and effectively hold bioactive cytokines and growth factors, like platelet-derived growth factor (PDGF) and transforming growth factor beta (TRG-β), which are produced during the initial phases of wound healing for the later phases. In addition, compared to delayed biodegradation of the remained clotting by fibrin glue as shown in Fig. 6b, the proper biodegradation of LAMBA can release the regeneration factors

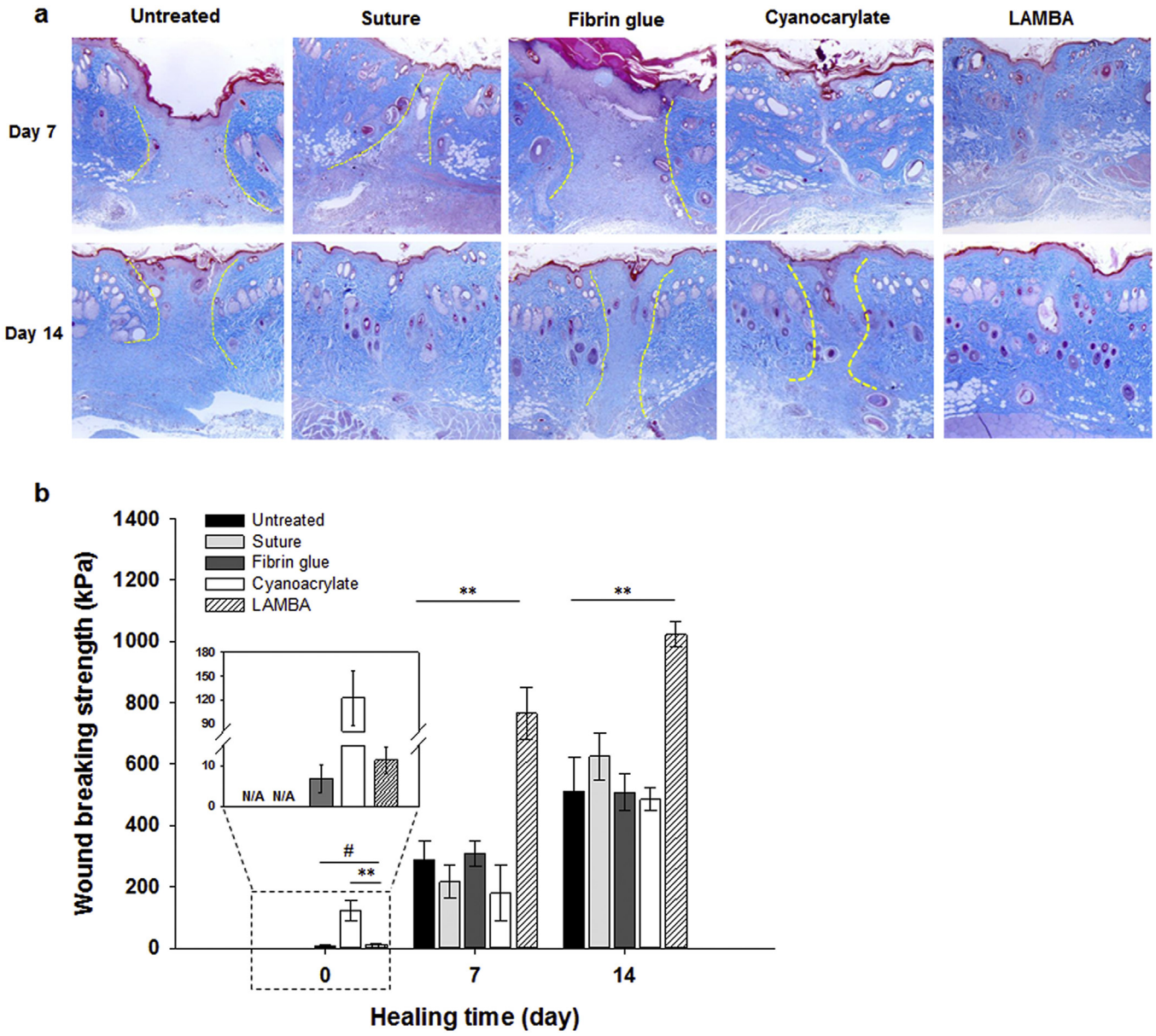

Fig. 7. a) Images of MT stained wounded tissues untreated or treated with suture, fibrin glue, cyanoacrylate and LAMBA at day 7 and 14 after treatment. Wound site (yellow dashed-line) is indicated. b) Measurement of wound breaking strength for skin closed by the respective samples at days 0, 7, and 14. A magnification box shows the strength at day 0. Three independent samples were averaged to obtain each measurement (**$p < 0.01$, *$p < 0.05$, #$p > 0.05$). (For interpretation of the references to colour in this figure legend, the reader is referred to the web version of this article.)

which could interact with keratinocytes and fibroblasts prominent in the reparative dermis and stimulate production of collagen and ECM for wound remodeling.

Besides the visual analysis, the wound breaking strengths were measured (Fig. 7b). At day 0, the strengths of the cyanoacrylate-, fibrin glue-, and LAMBA-treated skins were 122.4 ± 34.5 kPa, 6.87 ± 3.49 kPa, and 11.33 ± 3.22 kPa, respectively. The initial high strength of cyanoacrylate was attributed to the widely spread rigid polymer surface around the wound area, which provided strong mechanical support unlike the other treatments covering only the incision. Therefore, at day 7, the removal of the cover resulted in only a slight increase (~1.5-fold) in the strength of cyanoacrylate-treated skin relative to significant enhancements of the others, especially LAMBA (~67.6-fold). At day 14, the LAMBA-closed skin showed the highest wound breaking strength (1023.6 ± 42.0 kPa); strengths of 624.4 ± 75.9 kPa, 508.5 ± 60.2 kPa, and 484.9 ± 37.9 kPa were observed for sutures, fibrin glue, and cyanoacrylate, respectively. This high strength was likely due to the effective wound sealing of LAMBA; light-controllable crosslinking may enable surface adhesion between LAMBA and nucleophilic groups of ECM proteins on tissues [18] as well as cohesive dityrosine crosslinks between the tyrosine residues of LAMBA. Additionally, collagen deposition may also preserve structural integrity of the wound [32,33] (i.e., an increased resistance to mechanical stress), as indicated in the MT staining.

4. Conclusions

In summary, an unmodified tyrosine-rich MAP-based tissue glue was fabricated as an adhesive hydrogel via dityrosine formation

using photochemical crosslinking. LAMBA could rapidly (<60 s) close a bleeding and open wound on the back of a rat with light-controllable gelation and effective adherence to the wound. LAMBA could also facilitate tissue regeneration with minimal inflammation. Thus, the convenient handling, tunable physical properties, strong wet tissue adhesiveness, and biocompatibility of LAMBA provide a promising practical option for sutureless wound closures on delicate organs and non-reachable inner tissues. The LAMBA system could be broadly applied to all medical practices ranging from hemostatic agent and waterproof sealant for vascular defects to tissue grafting for hernias and blocking air leaks and perforations in biomaterials.

Acknowledgments

Financial support was provided by the Marine Biotechnology program (Marine BioMaterials Research Center) funded by the Ministry of Oceans and Fisheries, Korea (D11013214H480000110). E.Y.J. was supported by Global PH.D Fellowship program (014H1A2A1019946) funded by the Ministry of Education, Korea.

References

[1] L.P. Bré, Y. Zheng, A.P. Pêgo, W. Wang, Taking tissue adhesives to the future: from traditional synthetic to new biomimetic approaches, Biomater. Sci. 1 (2013) 239–253.
[2] A. Duarte, J. Coelho, J. Bordado, M. Cidade, M. Gil, Surgical adhesives: systematic review of the main types and development forecast, Prog. Polym. Sci. 37 (2012) 1031–1050.
[3] Y.C. Tseng, Y. Tabata, S.H. Hyon, Y. Ikada, *In vitro* toxicity test of 2-cyanoacrylate polymers by cell culture method, J. Biomed. Mater. Res. 24 (1990) 1355–1367.
[4] D.H. Sierra, A.W. Eberhardt, J.E. Lemons, Failure characteristics of multiple-component fibrin-based adhesives, Biomed. Mater. Res. 59 (2002) 1–11.
[5] T. Taguchi, H. Saito, Y. Uchida, M. Sakane, H. Kobayashi, K. Kataoka, et al., Bonding of soft tissues using a novel tissue adhesive consisting of a citric acid derivative and collagen, Mater. Sci. Eng. C 24 (2004) 775–780.
[6] J.H. Waite, M.L. Tanzer, Polyphenolic substance of *Mytilus edulis*: novel adhesive containing L-dopa and hydroxyproline, Science. 212 (1981) 1038–1040.
[7] B.P. Lee, P.B. Messersmith, J.N. Israelachvili, J.H. Waite, Mussel-inspired adhesives and coatings, Annu. Rev. Mater. Res. 41 (2011) 99.
[8] H.J. Cha, D.S. Hwang, S. Lim, Development of bioadhesives from marine mussels, Biotechnol. J. 3 (2008) 631–638.
[9] D.S. Hwang, Y. Gim, H.J. Yoo, H.J. Cha, Practical recombinant hybrid mussel bioadhesive fp-151, Biomaterials. 28 (2007) 3560–3568.
[10] H. Zeng, D.S. Hwang, J.N. Israelachvili, J.H. Waite, Strong reversible Fe^{3+}-mediated bridging between dopa-containing protein films in water, Proc. Natl. Acad. Sci. 107 (2010) 12850–12853.
[11] B.-H. Choi, H. Cheong, Y.K. Jo, S.Y. Bahn, J.H. Seo, H.J. Cha, Highly purified mussel adhesive protein to secure biosafety for *in vivo* applications, Microb. Cell. Fact. 13 (2014) 52.
[12] J.J. Wilker, Biomaterials: redox and adhesion on the rocks, Nat. Chem. Biol. 7 (2011) 579–580.
[13] K. Marumo, J. Waite, Optimization of hydroxylation of tyrosine and tyrosine-containing peptides by mushroom tyrosinase, BBA-Protein Struct. M. 872 (1986) 98–103.
[14] C.M. Elvin, A.G. Carr, M.G. Huson, J.M. Maxwell, R.D. Pearson, T. Vuocolo, et al., Synthesis and properties of crosslinked recombinant pro-resilin, Nature. 437 (2005) 999–1002.
[15] D.J. Raven, C. Earland, M. Little, Occurrence of dityrosine in Tussah silk fibroin and keratin, BBA-Protein Struct. M. 251 (1971) 96–99.
[16] S.O. Andersen, The cross-links in resilin identified as dityrosine and trityrosine, Biochim. Biophys. Acta 93 (1971) 213–215.
[17] K. Stewart, P. Spedding, M. Otterburn, D. Lewis, Surface layer of wool. II. Dityrosine in wool, J. Appl. Polym. Sci. 66 (1997) 2365–2376.
[18] D.A. Fancy, T. Kodadek, Chemistry for the analysis of protein–protein interactions: rapid and efficient cross-linking triggered by long wavelength light, Proc. Natl. Acad. Sci. 96 (1999) 6020–6024.
[19] J. Fang, H. Li, A facile way to tune mechanical properties of artificial elastomeric proteins-based hydrogels, Langmuir 28 (2012) 8260–8265.
[20] H. Shin, J.S. Temenoff, A.G. Mikos, *In vitro* cytotoxicity of unsaturated oligo [poly (ethylene glycol) fumarate] macromers and their cross-linked hydrogels, Biomacromolecules 4 (2003) 552–560.
[21] F. Couet, N. Rajan, D. Mantovani, Macromolecular biomaterials for scaffold-based vascular tissue engineering, Macromol. Biosci. 7 (2007) 701–718.
[22] K. Whang, K. Healy, D. Elenz, E. Nam, D. Tsai, C. Thomas, et al., Engineering bone regeneration with bioabsorbable scaffolds with novel microarchitecture, Tissue Eng. 5 (1999) 35–51.
[23] N.A. Peppas, J.Z. Hilt, A. Khademhosseini, R. Langer, Hydrogels in biology and medicine: from molecular principles to bionanotechnology, Adv. Mater. 18 (2006) 1345–1360.
[24] K. Miller, K. Chinzei, G. Orssengo, P. Bednarz, Mechanical properties of brain tissue *in-vivo*: experiment and computer simulation, J. Biomech. 33 (2000) 1369–1376.
[25] W.C. Yeh, P.C. Li, Y.M. Jeng, H.C. Hsu, P.L. Kuo, M.L. Li, et al., Elastic modulus measurements of human liver and correlation with pathology, Ultrasound. Med. Biol. 28 (2002) 467–474.
[26] T.A. Krouskop, T.M. Wheeler, F. Kallel, B.S. Garra, T. Hall, Elastic moduli of breast and prostate tissues under compression, Ultrason. Imaging. 20 (1998) 260–274.
[27] Q. Lu, E. Danner, J.H. Waite, J.N. Israelachvili, H. Zeng, D.S. Hwang, Adhesion of mussel foot proteins to different substrate surfaces, J. R. Soc. Interface. 10 (2013) 20120759.
[28] Q. Lu, D.X. Oh, Y. Lee, Y. Jho, D.S. Hwang, H. Zeng, Nanomechanics of cation–π interactions in aqueous solution, Angew. Chem. Int. Ed. 52 (2013) 3944–3948.
[29] D.S. Hwang, H. Zeng, Q. Lu, J. Israelachvili, J.H. Waite, Adhesion mechanism in a DOPA-deficient foot protein from green mussels, Soft. Matter 8 (2012) 5640–5648.
[30] C.M. Elvin, T. Vuocolo, A.G. Brownlee, L. Sando, M.G. Huson, N.E. Liyou, et al., A highly elastic tissue sealant based on photopolymerised gelatin, Biomaterials. 31 (2010) 8323–8331.
[31] G.J. Clydesdale, G.W. Dandie, H.K. Muller, Ultraviolet light induced injury: immunological and inflammatory effects, Immunol. Cell. Biol. 79 (2001) 547–568.
[32] R.F. Diegelmann, M.C. Evans, Wound healing: an overview of acute, fibrotic and delayed healing, Front. Biosci. 9 (2004) 283–289.
[33] S. Baranoski, E.A. Ayello, Wound Care Essentials: Practice Principles, Lippincott Williams & Wilkins, 2008, p. 120.